

## Scanning transmission electron microscopy investigation of the Si(111)/AlN interface grown by metalorganic vapor phase epitaxy

G. Radtke,<sup>1,a)</sup> M. Couillard,<sup>2</sup> G. A. Botton,<sup>2</sup> D. Zhu,<sup>3</sup> and C. J. Humphreys<sup>3</sup>

<sup>1</sup>IM2NP, UMR 6242 CNRS, Faculté des Sciences de Saint-Jérôme, Case 262, 13397 Marseille Cedex 20, France

<sup>2</sup>Brockhouse Institute for Material Research and Canadian Centre for Electron Microscopy, McMaster University, 1280 Main St. West, Hamilton, Ontario L8S 4M1, Canada

<sup>3</sup>Department of Materials Science and Metallurgy, University of Cambridge, Pembroke Street, Cambridge CB2 3QZ, United Kingdom

(Received 2 November 2010; accepted 23 November 2010; published online 20 December 2010)

The structure and chemistry of the interface between a Si(111) substrate and an AlN(0001) thin film grown by metalorganic vapor phase epitaxy have been investigated at a subnanometer scale using high-angle annular dark field imaging and electron energy-loss spectroscopy.  $\langle 11\bar{2}0 \rangle_{\text{AlN}} \parallel \langle 110 \rangle_{\text{Si}}$  and  $\langle 0001 \rangle_{\text{AlN}} \parallel \langle 111 \rangle_{\text{Si}}$  epitaxial relations were observed and an Al-face polarity of the AlN thin film was determined. Despite the use of Al deposition on the Si surface prior to the growth, an amorphous interlayer of composition  $\text{SiN}_x$  was identified at the interface. Mechanisms leading to its formation are discussed. © 2010 American Institute of Physics. [doi:10.1063/1.3527928]

The growth of GaN based nanostructures on Si has become a very active field of research particularly for the development of light emitting diodes. The choice of Si is motivated by the large-area size of the wafers available for this material, its high crystal quality, electric and thermal conductivities, and its low cost. The direct growth of GaN on Si(111) is, however, greatly hindered by a large mismatch in lattice parameters (17%) and thermal expansion coefficients usually resulting in a poor crystal quality of the GaN film. The growth of an intermediate AlN buffer layer appears as an interesting solution to circumvent this difficulty and achieve high-quality GaN layers on Si wafers. Reports on the low temperature growth by molecular beam epitaxy<sup>1</sup> and metalorganic vapor phase epitaxy (MOVPE)<sup>2</sup> of AlN on Si(111) reveal the presence of an atomically sharp interface where a periodic array of misfit dislocations accommodates the large lattice mismatch existing between AlN(0001) and Si(111) surfaces. However, most of the structural investigations performed on materials grown at high temperature ( $>1010$  °C) by MOVPE report the presence of an interlayer at the AlN/Si interface, generally assigned to amorphous  $\text{SiN}_x$ .<sup>3–7</sup> Al predeposition on the Si surface prior to the growth of the AlN thin film has been shown to prevent the formation of  $\text{SiN}_x$ , at least at the early stage of growth,<sup>8</sup> and is now widely utilized for this purpose. Interestingly, a number of studies in which this procedure has been carried out still report the presence of an amorphous interlayer. Its origin has been attributed either to an interdiffusion between the Si substrate and the AlN thin film during the growth<sup>4,9</sup> or to a stress relaxation mechanism.<sup>7</sup> As this interface largely determines the structural quality of the AlN buffer and therefore of the subsequently deposited GaN based nanostructures, it is of crucial importance to investigate the structure and chemistry of this interlayer at a subnanometer scale and to unravel the mechanisms leading to its formation.

In this letter, based on aberration corrected scanning transmission electron microscopy, we report a high reso-

lution study of the structure and chemistry of the Si(111)/AlN interface grown at high temperature by MOVPE. Experimental results suggest that, despite the predeposition of Al, a strong reaction between N and Si occurring at the beginning of the growth leads to the formation of the amorphous  $\text{SiN}_x$  layer at the interface.

All the samples were grown on 2 in. Si (111) substrates by MOVPE in a  $6 \times 2$  in.<sup>2</sup> Aixtron close-coupled showerhead reactor. Trimethylaluminum (TMA) was used as a group-III precursor, while ammonia was used as the nitrogen source. The as-supplied Si (111) substrate was first annealed in the reactor at 1100 °C under hydrogen ambient to remove the native oxide layer. The temperature was then decreased to 1040 °C for a 2 s TMA pre-dose, followed by the growth of an initial AlN layer at the same temperature for 30 s. After the initiation layer, the growth temperature was raised to 1100 °C for the growth of the main AlN epilayer at growth rates of up to 0.3  $\mu\text{m}/\text{h}$  and V/III ratio of  $\sim 2400$ . The reactor pressure for AlN growth was 50 Torr and the total thickness of the AlN layer was  $\sim 200$  nm. Cross-sectional transmission electron microscopy specimens were prepared by wedge mechanical polishing until electron transparency. The surface was subsequently cleaned using low tension Ar-ion milling (300 V for 10 min and 150 V for 10 min) just before inserting the sample in the microscope. The data shown hereafter were acquired on a FEI-Titan 80-300 cubed electron microscope operated at 300 keV and equipped with an aberration corrector of the probe-forming lens, an electron beam monochromator, an aberration corrector of the imaging lens, and a Gatan model 866 imaging filter. The convergence semiangle was set to 24 mrad for imaging, achieving a sub-angstrom probe, and to 18 mrad for spectroscopic measurements.

Figure 1(a) shows a characteristic low magnification high-angle annular dark field (HAADF) image of the Si(111)/AlN interface. An amorphous interlayer, corresponding to the dark area between the substrate and the film, is observed along the interface with a thickness varying between 1.5 and 2 nm. A high resolution HAADF image of this

<sup>a)</sup>Electronic mail: guillaume.radtke@im2np.fr.

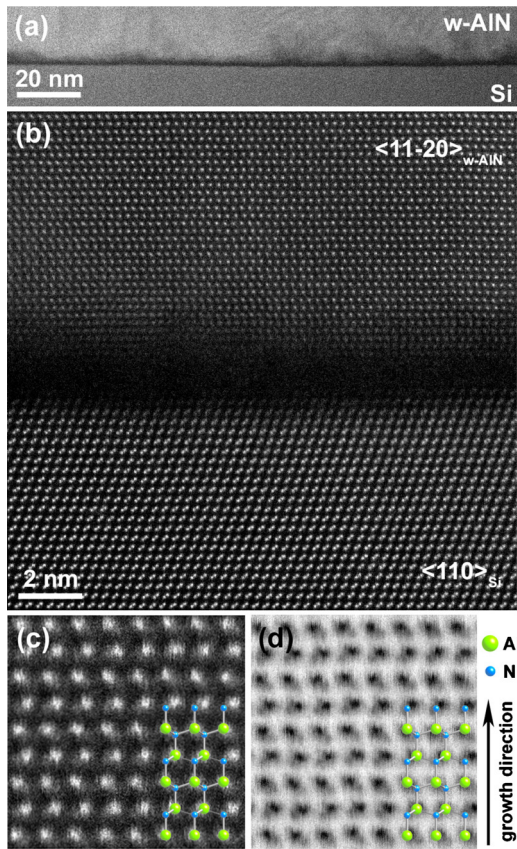


FIG. 1. (Color online) (a) Low-magnification HAADF view of the Si(111)/AlN interface. (b) High-resolution HAADF image of the interface acquired in the  $\langle 110 \rangle$  zone axis of the Si wafer. (c) Detail of the atomic structure of the film showing the Al-polarity of AlN observed in HAADF and (d) in ABF.

interface, acquired with a 75 mrad ADF inner angle in the Si  $\langle 110 \rangle$  zone axis is displayed in Fig. 1(b). Interestingly, despite the presence of this continuous layer, the epitaxial relations  $\langle 11\bar{2}0 \rangle_{\text{AlN}} \parallel \langle 110 \rangle_{\text{Si}}$  and  $\langle 0001 \rangle_{\text{AlN}} \parallel \langle 111 \rangle_{\text{Si}}$  are fairly well respected. A detailed investigation of the atomic structure of AlN, shown in Fig. 1(c), reveals the Al-face polarity of the film. The short Al–N interatomic distance in this projection (1.1 Å) and the presence of the neighboring strongly scattering Al make the N appear as an elongation of the Al alternatively pointing diagonally left and right. For comparison, an image of the same area acquired in annular bright field (ABF) with a 12–26 mrad detector, allowing a better visibility of the light N atomic columns,<sup>10</sup> is displayed in Fig. 1(d) and confirms the Al-face polarity of the thin film.

In a second step, the chemical analysis of this interface was carried out using electron energy-loss spectroscopy (EELS) spectrum imaging. Figure 2 shows the two-dimensional maps obtained from a  $175 \times 36$  pixels spectrum-image acquired at 300 keV without drift correction, a dwell time of 30 ms/pixel, and a collection semiangle of 80 mrad. Figure 2(a) shows the HAADF image acquired simultaneously with the EELS spectra. Figures 2(b)–2(d) show, respectively, the Si, N, and Al maps obtained by multiple linear least squares fit of the spectrum-image with reference spectra acquired in the same conditions. This procedure was required for a proper extraction of the Al and Si signals from their overlapping  $L_{23}$  edges. Finally, Fig. 2(e) shows the elemental profiles obtained by integrating the signal perpen-

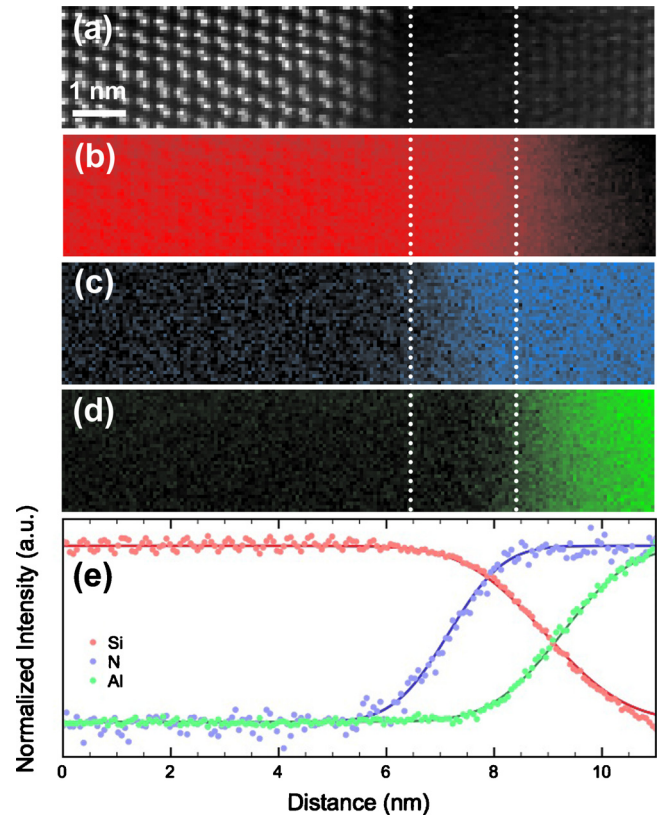


FIG. 2. (Color online) EELS spectrum-image of the Si(111)/AlN interface: (a) HAADF image, (b) Si map extracted from the Si- $L_{23}$  edge (99 eV), (c) N map extracted from the N-K edge (401 eV), (d) Al map extracted from the Al- $L_{23}$  edge (77 eV), and (e) EELS profiles obtained by integrating the signal perpendicularly to the interface. The dotted lines represent the approximate position of the interfacial layer.

dicularly to the interface and normalized to their maximum height. Note that no detectable O signal was recorded in this area. As these experiments were performed with a probe size of about 1 Å, the broad distribution of the chemical profiles presented here is intrinsic to the sample and does not arise from an experimental broadening. This chemical analysis confirms that the amorphous zone observed in the HAADF at the interface corresponds to a  $\text{SiN}_x$  layer. The chemical profiles shown in Fig. 2(e) bring, however, further information. First, the distribution of Si (3 nm wide) extends beyond the  $\text{SiN}_x$  interlayer into the AlN film. This signal can be attributed either to overlapping AlN and  $\text{SiN}_x$  signals over the thickness of the specimen or to a heavily doped AlN intermediate phase. Second, the profiles of N and Al, respectively, 2 and 2.5 nm wide, are similar but shifted with respect to each other by 1.8 nm. A non-negligible Al signal is therefore only observed above the  $\text{SiN}_x$  interlayer, in the AlN film.

In order to confirm our analysis of the interlayer, energy-loss near edge structures (ELNESS) of the Si- $L_{23}$ , Al- $L_{23}$ , and N-K edges, displayed in Fig. 3, were recorded for the three phases with a high-energy resolution ( $\sim 0.3$  eV) in monochromated mode. Whereas the signatures recorded in the Si substrate and the AlN thin film exhibit very fine structures characteristic of the bulk references,<sup>11,12</sup> the ELNESS acquired in the interlayer are much broader, as expected for a substoichiometric amorphous material. The chemical shift observed on the Si- $L_{23}$  edge between the interlayer and the Si substrate ( $2.5 \pm 0.5$  eV), attributed in first approximation to a charge transfer from Si to N atoms, also appears as a direct

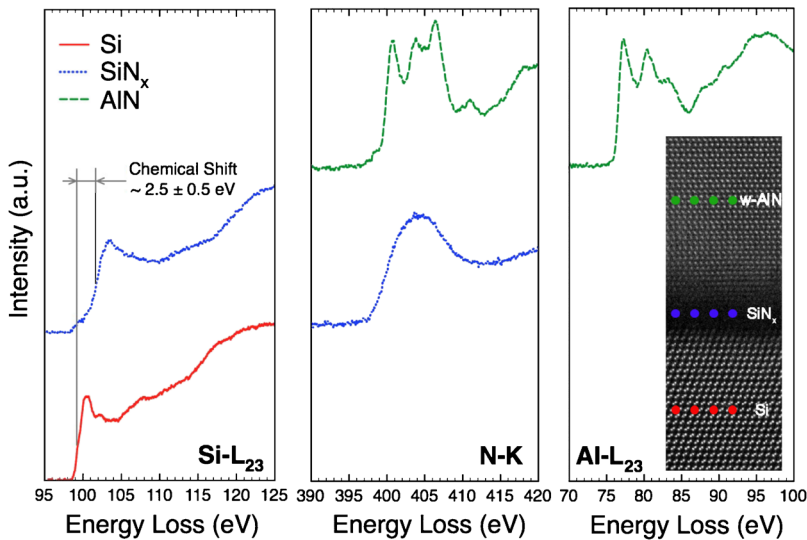


FIG. 3. (Color online) High-energy resolution ELNES obtained from bulk Si (solid line), bulk AlN (dashed line), and from the interfacial layer (dotted line). The spectra displayed here are the sum of spectra acquired by scanning the probe parallel to the interface as indicated by the dots in the inset.

evidence for the formation of Si–N chemical bonds in the amorphous phase.

Our chemical analysis of the interface shows that Al pre-deposition is unable to prevent the strong reaction occurring between N and the Si substrate, at least at high temperatures. Elemental profiles across the interface favor the hypothesis of the formation of the SiN<sub>x</sub> layer underneath the surface at the very beginning of the growth. An Al and Si rich surfactant layer could indeed form simultaneously, owing to their relatively low surface energies ( $\sim 1200$  mJ/m<sup>2</sup>). This is supported by the large proportion of Si found above the amorphous layer and by the absence of detectable Al in the Si wafer and the SiN<sub>x</sub> region. After reaching a critical thickness, the SiN<sub>x</sub> layer acts as a barrier, considerably slowing down the diffusion of Si from the wafer toward the surface. The increasing concentration of Al at the surface would then trigger the growth of the AlN thin film. The same analysis has been carried out on a 20 nm thick AlN epilayer sample grown under the same conditions for a shorter time ( $\sim 4$  min). The observation of an amorphous interlayer with the same characteristics further supports the hypothesis of a rapid formation of SiN<sub>x</sub> as a first step of the growth process. Within this framework, the crystallographic relationship between the AlN layer and the Si substrate, as well as the Al-face polarity of the film, also reported previously in the presence of a sharp Si(111)/AlN interface,<sup>2</sup> remains unexplained. Different hypotheses have been formulated to clarify this point, particularly in the case of growths preceded by a nitridation step.<sup>13</sup> A plausible explanation resides in the presence of contact points between the Si substrate and the AlN film due to discontinuities in the SiN<sub>x</sub> interlayer.

Electron microscopy was carried out at the Canadian Centre for Electron Microscopy, a facility supported by the NSERC (Canada) and McMaster University. C.J.H. and G.A.B. are grateful for funding from the Ministry of Research and Innovation of Ontario (ISOP program). G.R. and G.A.B. acknowledge the Fonds France-Canada pour la Recherche for partial support of this collaboration. G.R. thanks A. Saul (CINaM-CNRS, Marseille) for helpful discussions.

- <sup>1</sup>A. Bourret, A. Barski, J. L. Rouvière, G. Renaud, and A. Barbier, *J. Appl. Phys.* **83**, 2003 (1998).
- <sup>2</sup>R. Liu, F. A. Ponce, A. Dadgar, and A. Krost, *Appl. Phys. Lett.* **83**, 860 (2003).
- <sup>3</sup>K. Y. Zang, S. J. Chua, L. S. Wang, and C. V. Thompson, *Phys. Status Solidi C* **0**, 2067 (2003).
- <sup>4</sup>S.-J. Lee, S.-H. Jang, S.-S. Lee, and C.-R. Lee, *J. Cryst. Growth* **249**, 65 (2003).
- <sup>5</sup>S. Tanaka, Y. Kawaguchi, N. Sawaki, M. Hibino, and K. Hiramoto, *Appl. Phys. Lett.* **76**, 2701 (2000).
- <sup>6</sup>S. Kaiser, M. Jakob, J. Zweck, W. Gebhardt, O. Ambacher, R. Dimitrov, A. T. Schremer, J. A. Smart, and J. R. Shealy, *J. Vac. Sci. Technol. B* **18**, 733 (2000).
- <sup>7</sup>G. Q. Hu, X. Kong, L. Wan, Y. Q. Wang, X. F. Duan, Y. Lu, and X. L. Liu, *J. Cryst. Growth* **256**, 416 (2003).
- <sup>8</sup>K. Y. Zang, L. S. Wang, S. J. Chua, and C. V. Thompson, *J. Cryst. Growth* **268**, 515 (2004).
- <sup>9</sup>D. Xi, Y. Zheng, P. Chen, Z. Zhao, P. Chen, S. Xie, B. Shen, S. Gu, and R. Zhang, *Phys. Status Solidi A* **191**, 137 (2002).
- <sup>10</sup>S. D. Findlay, N. Shibata, H. Sawada, E. Okunishi, Y. Kondo, T. Yamamoto, and Y. Ikuhara, *Appl. Phys. Lett.* **95**, 191913 (2009).
- <sup>11</sup>V. Serin, C. Colliex, R. Brydson, S. Matar, and F. Boucher, *Phys. Rev. B* **58**, 5106 (1998).
- <sup>12</sup>P. E. Batson, *Phys. Rev. B* **47**, 6898 (1993).
- <sup>13</sup>E. Arslan, M. K. Ozturk, Ö. Duygulu, A. Arslan Kaya, S. Ozcelik, and E. Ozbay, *Appl. Phys. A: Mater. Sci. Process.* **94**, 73 (2009).